Supplementary Figure Legends

Figure S1. Characterization of CCK2R-BAC-CreERT mice.

(A) Gene construct of CCK2R-BAC-CreERT mice and Rosa26rTdTomato or Rosa26rmTmG reporter mice. (B and C) CCK2R-BAC-CreERT2;Rosa26rTdTomato mice were given 6 mg tamoxifen and sacrificed after 24 hours. Immunofluorescence of H/K-ATPase (B), chromogranin A (ChgA) (C), and gastric intrinsic factor (GIF) (D) with labelled red cells in the corpus is shown. (E-H) Immunofluorescence of Dclk1 (E), gastrin (F), TFF1 (G), somatostatin (H) with labelled red cells in the antrum at day1 tamoxifen induction is shown. (I) Ratio of ChgA cells in labelled CCK2R+ cells or CCK2R-EGFP+ cells. (J and K) Mice were given 6 mg tamoxifen and sacrificed after 24 hours. H&E staining (J, antrum) and cleaved caspase-3 staining (K, antrum and corpus) are shown. (L) Day30 lineage tracing of CCK2RCreERT;Rosa26rTdTomato mouse antrum after 1 mg tamoxifen administration.

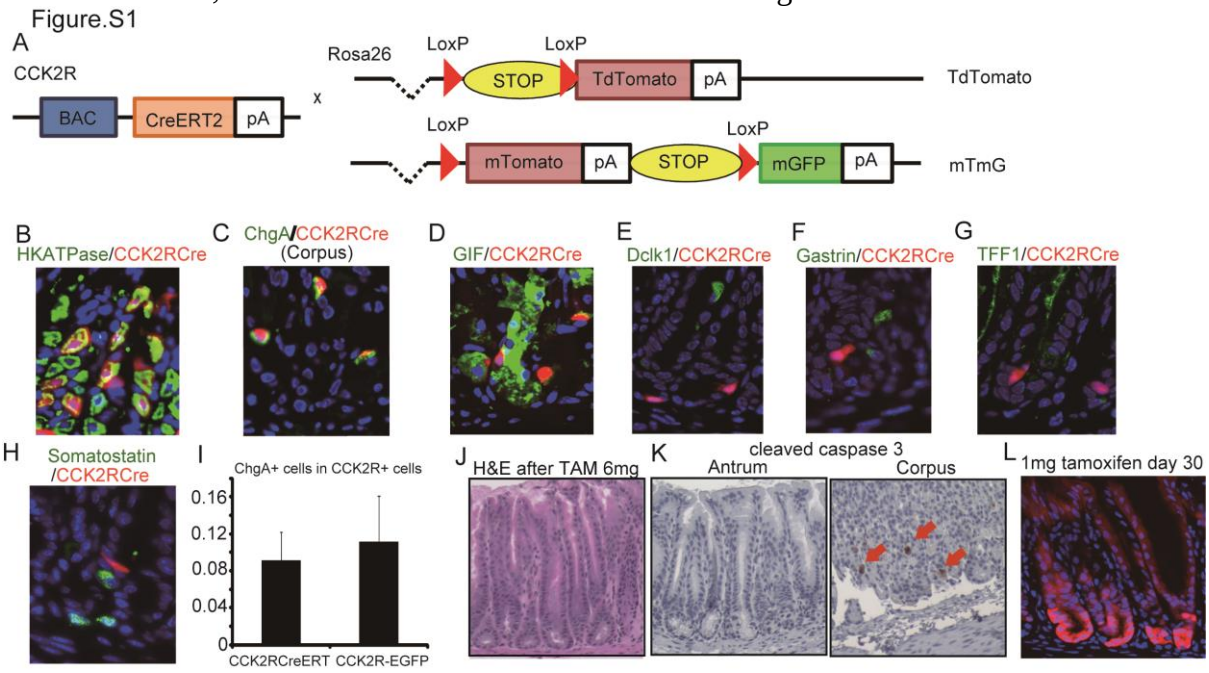

Figure S2. Proliferation, Lgr5 expression, and colony formation ability in CCK2R+ cells and ChgA+ cells under progastrin overexpression.

(A) Double staining of Ki67 (red) and ChgA (green) in WT and hGAS mouse antrum. (B) ChgA staining (red) of Lgr5-GFP and Lgr5-GFP;hGAS mouse antrum. (C) Ki67 staining (red) of CCK2RCreERT;hGAS;Rosa26rmTmG mouse antrum 24 hours after tamoxifen. Recombined cells were stained by GFP antibody. (D) The percentage of Ki67+ cells in totalCCK2R+ cells in CCK2RCreERT;Rosa26rmTmG mouse and CCK2RCreERT;hGAS; Rosa26rmTmG mouse antrum. (E) Single cell culture colony formation efficiency (%) of $Lgr5_{low}$ cells with or without progastrin/YF476.

Figure.S2

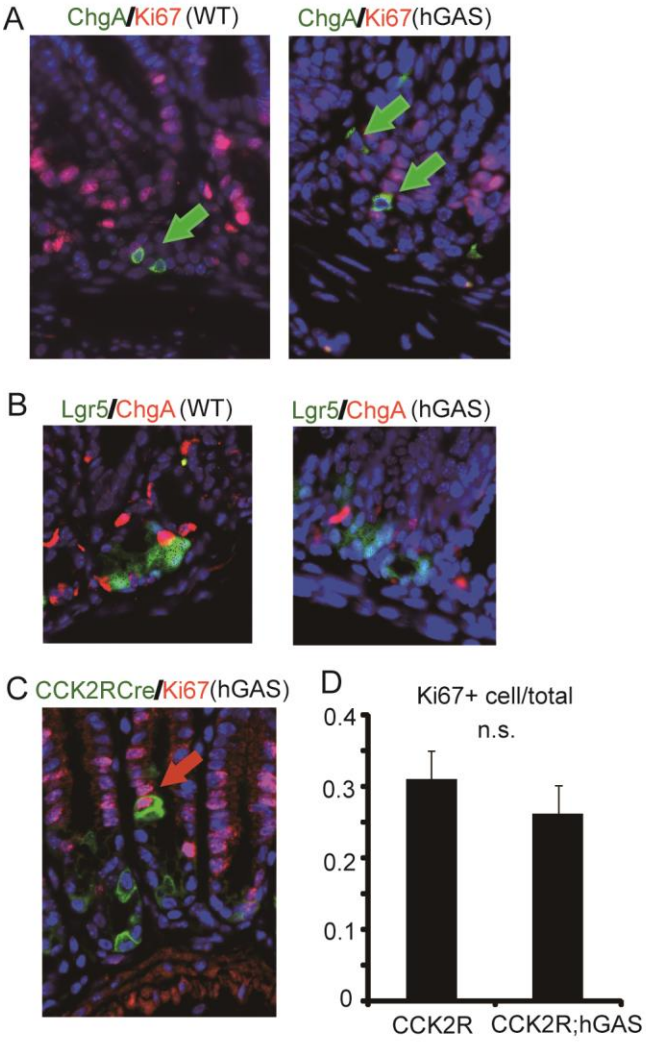
A
ChgA/Ki67 (WT)
ChgA/Ki67(hGAS)
B
Lgr5/ChgA (WT)
Lgr5/ChgA (hGAS)
C CCK2RCre/Ki67(hGAS)
D
Ki67+ cell/total
n.s.
0.4
0.3
0.2
0.1
0
CCK2R
CCK2R;hGAS
E
%colony formation
2
1
0
control
progastrin
progastrin YF476

Figure S3. The gastric histology, the gastric acid secretion, Lgr5 expression, and serum levels of progastrin in the stomachs of WT and hGAS mice.
(A) H&E image of the gastric corpus and antrum of aged WT and hGAS mice (21-month old) without treatment (magnification: x40). (B) The gastric acid output of hGAS (n=3) and WT (n=3) mice without treatment (3 month old). The gastric acid output was measured by pyloric ligation method. The acidity of the gastric contents was measured by titration with 0.01N NaOH and expressed as H+ μan. (C) Representative GFP staining of Lgr5-GFP and Lgr5-GFP;hGAS mice without MNU treatment. (D) Serum progastrin levels of WT and hGAS mice with or without MNU and *H.felis* treatment (n=3, each group).

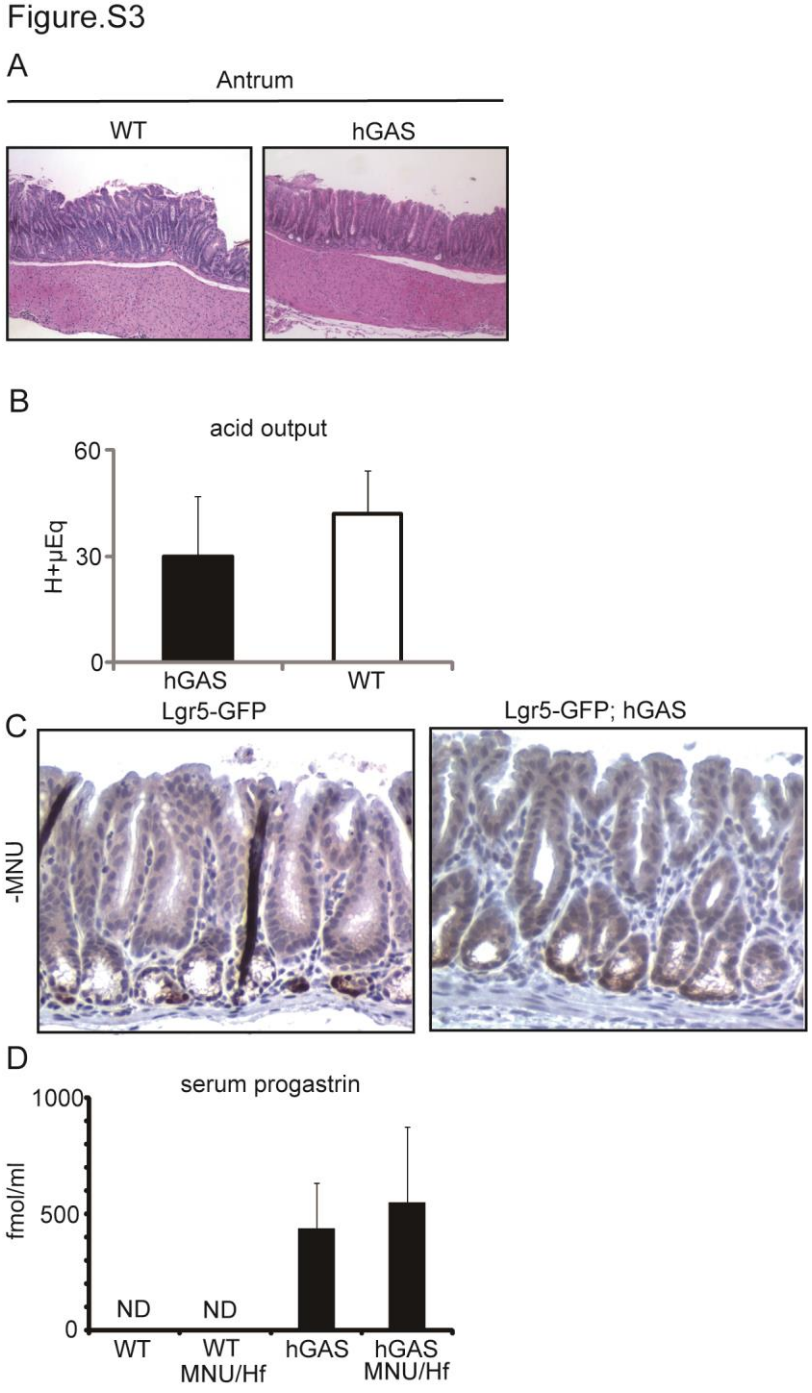

Figure S4. Progastrin promotes MNU-induced antral carcinogenesis.

(A) WT and hGAS mice were treated with MNU and *H. felis*, and sacrificed at 12 weeks after the beginning of MNU. Representative H&E (x 100), Ki67 (x 200), and CD44 (x100) staining images are shown. (B) GAPDH-normalized expression of the CD44 gene in the stomachs of WT and hGAS with or without MNU treatment (n=3 for each group). Relative expression in uninfected WT mice is represented as 1.0. Data are plotted as the means ± S.E. (*p<0.05).

Figure.S4

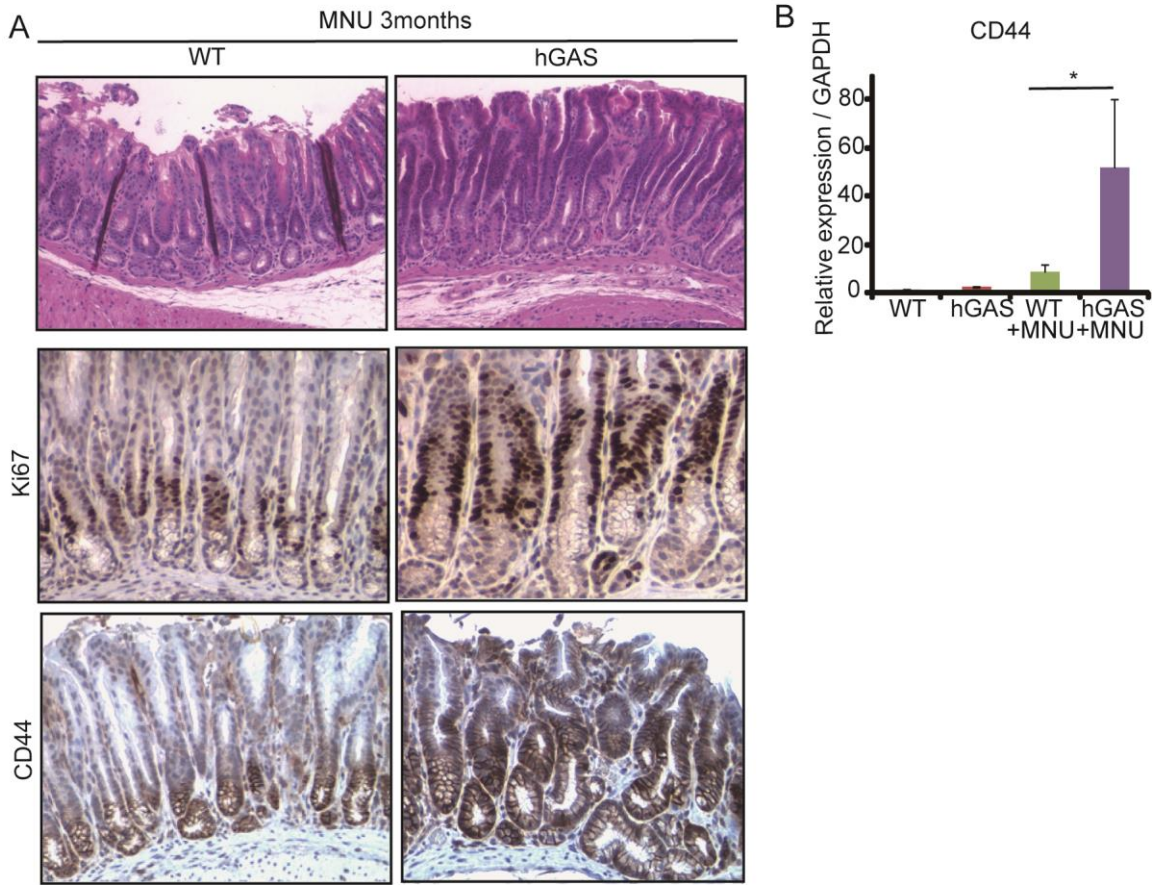

Figure S5. Progastrin increases CCK2R-lineage tracing *in vitro.*
(A) CCK2R-BAC-CreERT2;Rosa26r-mTmG mice were given 6 mg tamoxifen and sacrificed after 24 hours. Antral glands were isolated and applied for 3D culture. Representative time course of the identical organoids with or without progastrin. (B) More than 50% labeled organoid number was counted (n=4), and percentages in total GFP+ organoids are plotted as the means ± S.E. (*p<0.05).

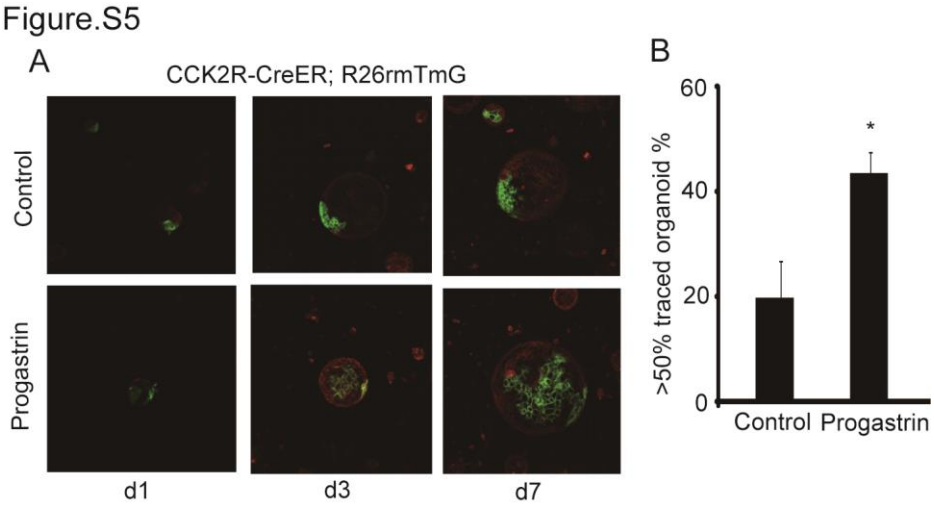

Figure S6. Protocol of YF476 treatment.
(A) Protocol of YF476 treatment in early phase during MNU/*H.felis* exposure.
(B) Protocol of YF476 treatment in late phase of MNU/*H.felis* exposure.

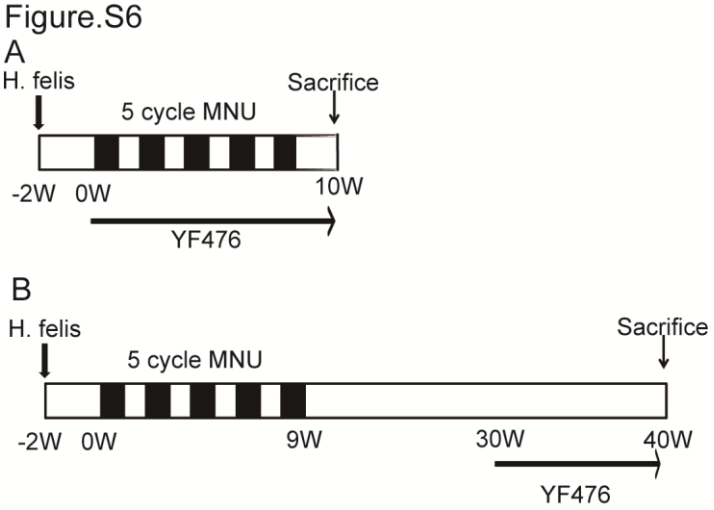

Figure S7. Lgr5+ cells after CCK2R gene ablation.
Representative GFP expression in the antrum of non-treated Lgr5-GFP;hGAS;CCK2R$^{+/-}$mice and Lgr5-GFP;hGAS;CCK2R$^{-/-}$ mice.

Figure. S7

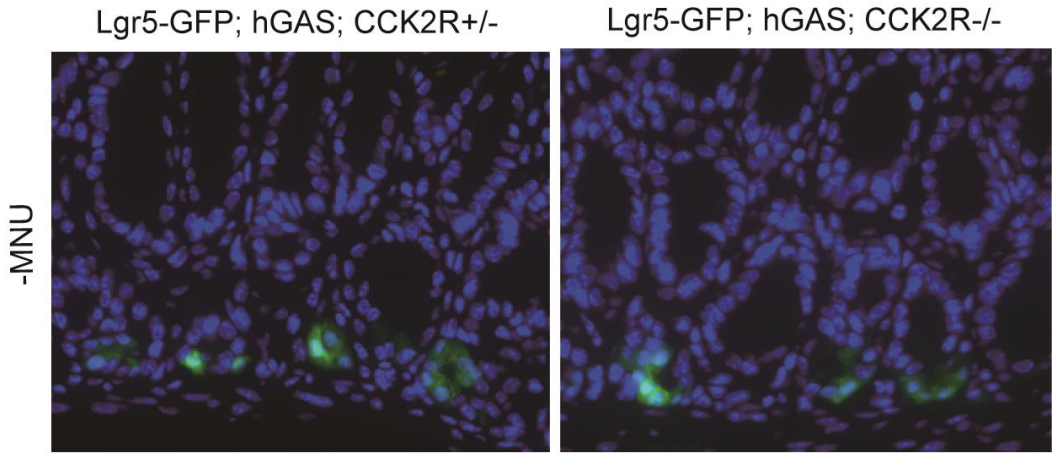

Figure S8. Progastrin promotes *H. felis*-induced antral carcinogenesis.
(A, B) Gross appearance (A) and H&E images (B) of the antral mucosa of *H. felis*-infected WT and hGAS mice at 18 MPI (all B6 background). (C) The number of Ki67-positive cells in the gastric antrum was measured at 20 different locations in the each of 2 group mice (n=3). All values were expressed as mean ± SE ($p < 0.05$). (D, E) Immunohistochemistry of Ki67 (D) and CD44 (E) staining of the antrum of WT and hGAS mice.

Figure. S8

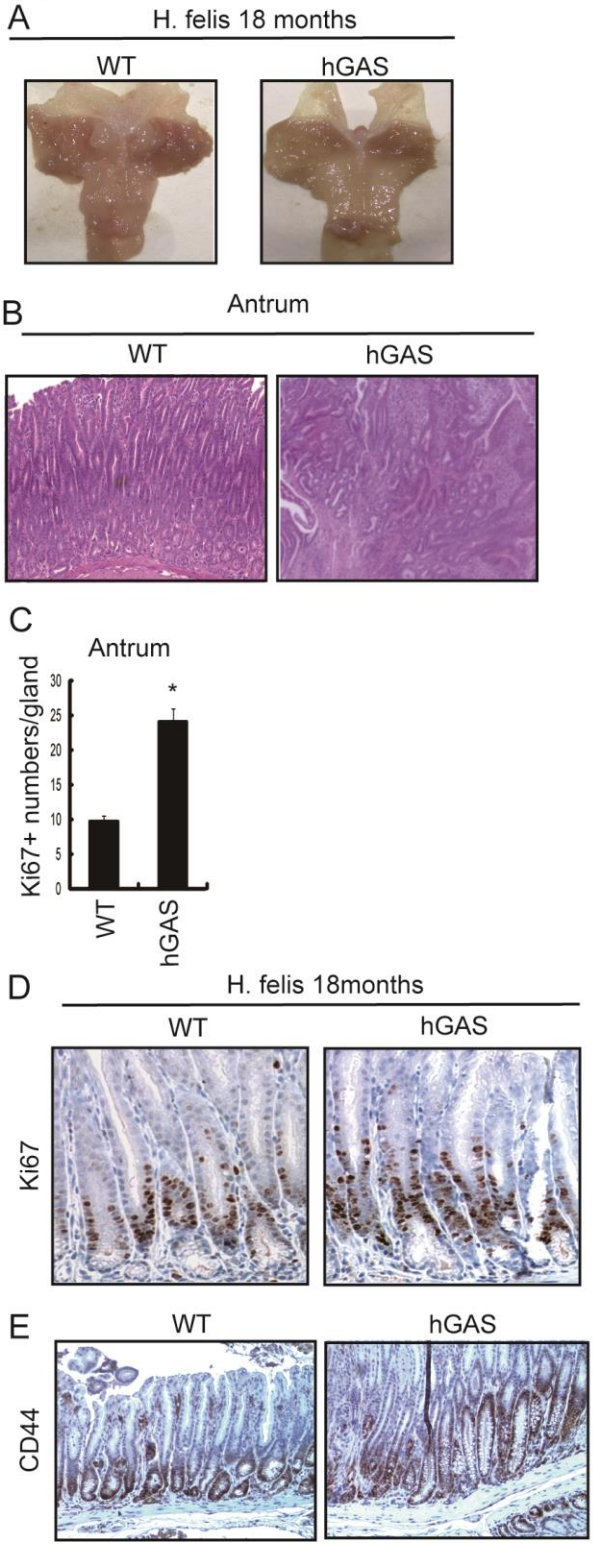
A
H. felis 18 months
WT
hGAS
B
Antrum
WT
hGAS
C
Antrum
Ki67+ numbers/gland
30
25
20
15
10
5
0
*
WT
hGAS
D
H. felis 18months
WT
hGAS
Ki67
E
WT
hGAS
CD44

Figure S9. Colocalization of Sox2 and CCK2R.
CCK2R-BAC-CreERT2;Rosa26rTdTomato mice were given 6 mg tamoxifen and sacrificed after 24 hours. Immunofluorescence of Sox2 with labelled red cells in the antrum is shown

Figure.S9